NOTE: This is the accepted version of the paper, to appear in IEEE Transactions on Magnetics.

# Improvised Asymptotic Boundary Conditions for Electrostatic Finite Elements

David Meeker, *Member, IEEE*

*Abstract*—**Improvised Asymptotic Boundary Conditions are a sparse but approximate method of solving open boundary problems. Since this method approximates unbounded space as series of isotropic shells, it can be readily implemented in virtually any finite element solver without the need for additional code. Previous work addressed application of this technique to magnetic problems described with a vector potential formulation. The present work extends the method to electrostatics and related scalar potential formulations.**

## I. INTRODUCTION

**A**SYMPTOTIC boundary conditions are an established method of addressing "open boundary" problems in electrostatics [1]. This method applies boundary conditions that emulate the impedance of an unbounded space for low-order harmonics at a nearby computational boundary. Previously, this method has been applied to 2D [2] and axisymmetric [3] electrostatic problems. Previous works only considered first- and second-order boundary conditions, and code modifications are required to implement the asymptotic boundary conditions.

Improvised asymptotic boundary conditions (IABCs) work on the same principle as other realizations of asymptotic boundary conditions, by reproducing the impedance of an unbounded region for low-order harmonics. However, IABCs can be implemented in an ad-hoc fashion, without requiring code changes. These boundary conditions are realized by constructing a series of concentric rings with appropriately specified material properties about a circular computational boundary.

Previous work on IABCs concentrated on magnetostatic problems posed with a vector potential formulation and results were limited to third order [4]. The present work extends the formulation to scalar potential problems with the particular motivation of solving unbounded 2D and axisymmetric electrostatic problems. The results presented in this work allow the realization of IABCs of up to tenth order for scalar potential problems. Several examples demonstrate the utility and performance of the method.

## II. PROBLEM DEFINITION

At low frequency, the electric field is described by a subset of Maxwell's equations[5]:

$$\nabla \cdot \mathbf{D} = \rho_e \qquad (1)$$

$$\nabla \times \mathbf{E} = 0 \qquad (2)$$

D. Meeker is with QinetiQ North America, 350 Second Ave, Waltham, MA, 02451 USA e-mail: dmeeker@ieee.org.

$$\mathbf{D} = \epsilon \mathbf{E} \qquad (3)$$

where $\mathbf{E}$ is the electric field intensity; $\mathbf{D}$ is the electric flux density; $\rho_e$ is electric charge density and $\epsilon$ is the electric permittivity. The electric field can be defined in terms of electric potential, $V$, as:

$$\mathbf{E} = -\nabla V \qquad (4)$$

allowing (1) and (2) to be captured as the second-order partial differential equation:

$$-\nabla \cdot \epsilon \nabla V = \rho_e \qquad (5)$$

This work considers solution of (5) in the "far field" region where $\rho_e = 0$ and $\epsilon = \epsilon_o$, the permittivity of free space. In the far field region, (5) reduces to the Laplace equation:

$$-\epsilon_o \nabla^2 V = 0 \qquad (6)$$

Although electrostatics is the primary motivation for the present work, the results of this work apply equally well to other problem domains that are described by equations of identical form to (1)-(6): scalar potential magnetostatics, inviscid fluid flow, steady-state heat flow, and steady-state groundwater flow. [5]

If $\rho$ is defined to be the distance from a fixed origin, the open boundary problem can be thought of as the solution to (6) in a bounded circular region with a radius $\rho = R_o$ in the case where the boundary location $R_0 \rightarrow \infty$. For magnetic problems posed in terms of vector potential, $A$, it is usually sufficient to use open boundary conditions that define $A = 0$ at $R_o$. Problems are typically defined as a collection of currents acting on regions filled with various magnetic properties, and it is natural the currents be defined in such a way that the currents are conserved in the near-field domain. In the far field, the potential behaves like a dipole (or a collection of dipoles), and the magnetic energy converges to a constant value as $R_0 \rightarrow \infty$. However, magnetic potential is usually not defined in the near field; the $A = 0$ boundary condition at infinity is needed to define a problem with a unique solution.

For electrostatic problems, the situation is more complicated due to the presence of isolated charges in the electrostatic formulation. For 2D problems, the solution for $V$ due to a point charge (*i.e.* the infinite space Green's function [8] ) varies with the $\log(\rho)$ rather than converging to a constant voltage as $\rho \rightarrow \infty$. When there is a net charge in the near field, a homogeneous Dirichlet ($V = 0$) boundary condition at $R_o$ stores charges on the boundary surface at $R_o$ and the energy stored in the electrostatic field increases without bound as $R_o$ approaches infinity.

Charge density on a surface is proportional to the normal voltage gradient at the surface. A homogeneous Neumann boundary condition, $dV/d\rho = 0$, applied at $R_o$, assures that no charge can spuriously be stored "at infinity", forcing all charge to be conserved in the near field region. In the case where the charge can't be forced to be conserved locally (*i.e.* when a net charge is explicitly specified in the near field region with no near-field reference voltage), the problem is ill-posed per the Fredholm Alternative [6], and the homogeneous Neumann boundary case will not have a solution for any $R_o$. Since the Neumann boundary condition forces charge to be conserved locally leading to convergent stored energy and disallows solutions for ill-posed problems, a Neumann boundary should be employed as the "default" boundary condition type for 2D electrostatic open boundary problems. A Dirichlet boundary should only be used for 2D problems in the case in which a configuration of charges that sums to zero is defined *a priori*, but the potential is nowhere fixed in the near field region. In that case, it is appropriate to use a homogeneous Dirichlet condition, V=0, as $\rho \to \infty$ to uniquely define the solution, similar to the situation in magnetic potential problems.

For axisymmetric cases, however, the solution for the voltage due to a net charge does converge to zero as $\rho \to \infty$. The stored energy can be bounded in the case where there is charged stored "at infinity". For some axisymmetric problems, a Dirichlet boundary condition is needed that stores charge at infinity–for example, the computation of the capacitance of an isolated sphere. Alternatively, a Neumann boundary condition can be applied for problems in which it is desired that charges should sum to zero locally–for example, computing the force between two separated spheres [7].

Since the choice of a Dirichlet (grounded at infinity) or Neumann (insulated at infinity) boundary condition depends upon the particulars of the problem at hand, both cases will be considered in the subsequent development for both 2D and axisymmetric cases.

## III. 2D IMPROVISED ABCs

In polar coordinates, the general 2D solution for (6), assuming no net charge in the near-field, is [2]:

$$V(\rho, \phi) = \sum_{n=1}^{\infty} \frac{v_n(\phi)}{\rho^n} \tag{7}$$

where $\rho$ and $\phi$ are the radius and angle that define the polar coordinate system, as shown in Fig. 1. It can be noted that (7) satisfies both $V = 0$ and $dV/d\rho = 0$ as $\rho \to \infty$, so (7) can be used to generate both Neumann- and Dirichlet-type open boundary approximations. By differentiating (7) with respect to $\rho$, a relationship between voltage and its derivative with respect to $\rho$ can be stated:

$$\frac{\partial V_n}{\partial \rho} = -\frac{n V_n}{\rho} \tag{8}$$

where $V_n$ represents the vector potential contribution of the $n^{th}$ harmonic. Eq. (8) can be interpreted as a set of boundary conditions that the true unbounded solution must satisfy at $\rho = R$ where $R$ is the radius of a circular artificial computational outer boundary. Asymptotic Boundary Conditions

seek boundary conditions that satisfy (8) for a few low-order harmonics, assuming that higher-order harmonics have decayed to insignificance if a suitably large $R$ has been selected.

Improvised Asymptotic Boundary Conditions (IABCs) are a method of enforcing the satisfaction of (8) for low-numbered harmonics. IABCs assume that (8) can be satisfied for the first $N$ harmonics by creating a circular outer boundary and placing $N$ addition thin annular regions with isotropic permittivities $\epsilon_1 \ldots \epsilon_N$ outside the boundary. Either $V = 0$ or $dV/d\rho = 0$ can be applied on the outer edge of the shells. Applying $V = 0$ on the outer shell corresponds to a Dirichlet boundary at infinity; applying $dV/d\rho = 0$ on the outer shell corresponds to a Neumann condition at infinity. A representative illustration of an IABC is shown in Figure 1, which depicts the construction of a second-order IABC. The following development describes the process for the computation of $\epsilon_1 \ldots \epsilon_N$ that satisfy (8).
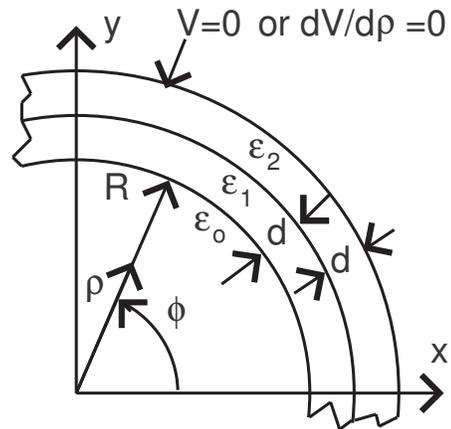


Fig. 1. Second order 2D planar improvised boundary condition.

The general solution for $V$ inside the $m^{th}$ shell can be represented in a separation-of-variables form as [8]:

$$V_m = \sum_{n=1}^{\infty} u_n(\rho) v_n(\phi) \tag{9}$$

where $m = 1 \ldots N$ indexes the layers in the boundary region and

$$u_n = c_{m1}(n)\rho^n + c_{m2}(n)\rho^{-n} \tag{10}$$

A system of $2N$ equations can then be written consisting of:

- One equation that fixes potential at the inner edge of the boundary region:

$$u_1(R) = 1 \tag{11}$$

- Two equations for each interface between layers in the boundary region. These equations represent the continuity of tangential field intensity and normal flux density, respectively:

$$u_m(R + m\,d) = u_{m+1}(R + m\,d) \tag{12}$$

$$\epsilon_1 \frac{\partial u_m}{\partial \rho}(R + m\,d) = \epsilon_2 \frac{\partial u_{m+1}}{\partial \rho}(R + m\,d) \tag{13}$$

- One equation defining the behavior at the outer edge of the boundary region. At the outer edge, the potential can be set to zero, corresponding a homogeneous Dirichlet condition ($V = 0$) at infinity:

$$u_N(R + Nd) = 0 \tag{14}$$

Alternatively, the normal gradient of potential can be set to zero at the outer edge, corresponding to a homogeneous Neumann condition ($dV/dr = 0$) at infinity.

$$\frac{du_N}{dr}(R + Nd) = 0 \tag{15}$$

For a given set of permittivities $\epsilon_1 \ldots \epsilon_2$ and layer thickness $d$ and radius $R$, eqs. (11)-(15) are a set of linear algebraic equations that are straightforward to solve for $c_{m1}(n)$ and $c_{m2}(n)$ for $m = 1 \ldots N$.

However, asymptotic boundary condition (8) applies on the $\rho = R_-$ side of the boundary. To move the boundary condition into the boundary region, continuity of the normal flux must be applied to yield:

$$\epsilon_0 \frac{\partial u}{\partial \rho}\Big|_{\rho=R_-} = \epsilon_1 \frac{\partial u_1}{\partial \rho}\Big|_{\rho=R_+} \tag{16}$$

Then, $N$ equations can be obtained by substituting (16) into (8) to each of the $N$ harmonics:

$$\frac{\epsilon_1}{\epsilon_o} \frac{\partial u_{1,n}}{\partial \rho}(R) + \frac{n u_{1,n}(R)}{R} = 0 \text{ for } n = 1 \ldots N \tag{17}$$

where $u_{1,n}$ denotes the solution for the $n^{th}$ harmonic in the first layer of the boundary. The shell permittivities, $\epsilon_1 \ldots \epsilon_N$ are determined by the selection of permittivities that satisfy (17).

The first-order case has simple solutions for $\epsilon_1$, but higher-order boundary conditions do not have simple analytical forms. For this paper, the built-in equation solvers in Mathematica were used to numerically solve (17), with solutions of (11)-(15) required for each harmonic to evaluate a trial solution of (17). For the purposes of a numerical solution, the solution is simplified if non-dimensional boundary layer thickness, defined as:

$$\delta = d/R \tag{18}$$

is employed.

The solution to the first-order 2D case with a Dirichlet ($V = 0$) outer boundary condition is:

$$\frac{\epsilon_1}{\epsilon_0} = \frac{\delta(\delta + 2)}{\delta^2 + 2\delta + 2} \approx \delta \tag{19}$$

and the solution the the first-order 2D case with a Neumann ($dV/dr = 0$) outer boundary condition is:

$$\frac{\epsilon_1}{\epsilon_0} = \frac{\delta^2 + 2\delta + 2}{\delta(\delta + 2)} \approx \frac{1}{\delta} \tag{20}$$

For higher-order cases, solutions over a range of $\delta$ are presented in Table I for a Dirichlet outer boundary and Table III for a Neumann outer boundary. Asymptotic expressions for the small $\delta$ case are presented as the first row in the table. The practically useful case of a $R/10$ total boundary region thickness are presented in Tables II and IV.

It can be noted that the relative permittivities for the Neumann case are the reciprocals of the relative permittivities for the Dirichlet case. The explanation for this relationship between the Neumann and Dirichlet cases can be seen by reformulating the far-field problem, eq. (6) in terms of electric vector potential instead of scalar potential. Denoting electric vector potential as $\mathbf{T}$, electric flux density is defined in terms of $\mathbf{T}$ as:

$$\mathbf{D} = \nabla \times \mathbf{T} \tag{21}$$

Applying the constitutive law of (3) and substituting into (2) gives a vector potential equation for the far field:

$$-\frac{1}{\epsilon}\nabla^2 \mathbf{T} = 0 \tag{22}$$

For the 2D case, the only non-zero element of $\mathbf{T}$ is the "out of the page" component $T_z$ so that (22) reduces to:

$$-\frac{1}{\epsilon}\nabla^2 T_z = 0 \tag{23}$$

Eq. (23) now has exactly the same form as (6), except that the reciprocal of permittivity (*i.e.* elasticity) appears in the place of permittivity.

If $T_z = 0$ is applied at an outer boundary, the condition $\mathbf{D} \cdot \mathbf{n}$ is at the boundary. This is exactly the same condition that is enforced by the selection of a $dV/d\rho = 0$ boundary condition in a scalar potential problem. That is, solving (23) subject to $T_z = 0$ at the outer edge is identical to solving (6) with $dV/d\rho = 0$ at the outer edge. Because of the similarity of the problems, the relative permittivities that enforce a Dirichlet boundary condition for a scalar potential formulation are the same as the relative elasticities that enforce a Dirichlet boundary condition for the vector potential formulation, explaining the reciprocal relationship for the permittivities for the Dirichlet and Neumann cases of the scalar potential IABC problem.

## IV. AXISYMMETRIC IMPROVISED ABCs

In polar coordinates, the general solution for voltage, $V$, on an unbounded domain is [3]:

$$V(\rho, \phi) = \sum_{n=0}^{\infty} \frac{v_n(\phi)}{\rho^{(n+1)}} \tag{24}$$

for the axisymmetric case, where $\rho$ is the the radial distance and $\phi$ is the polar angle in a spherical coordinate system. Unlike the 2D planar case, the axisymmetric problem has an $n = 0$ term corresponding to a net electric charge which must be considered for the Dirichlet outer boundary case.

By differentiating (7) with respect to $\rho$, it can be concluded that:

$$\frac{\partial V_n}{\partial \rho} = -\frac{(n+1)V_n}{\rho} \tag{25}$$

where $V_n$ represents the vector potential contribution of the $n^{th}$ harmonic.

For the axisymmetric case, the general solution for $V$ inside the $m^{th}$ shell is [9]:

$$V_m = \sum_{n=0}^{\infty} u_n(\rho)v_n(\phi) \tag{26}$$

TABLE I
HIGHER ORDER 2D SOLUTIONS WITH DIRICHLET OUTER BOUNDARY.

| $\delta$ | 2rd Order | | 3rd Order | | | 4th Order | | | |
|---|---|---|---|---|---|---|---|---|---|
| | $\epsilon_1/\epsilon_o$ | $\epsilon_2/\epsilon_o$ | $\epsilon_1/\epsilon_o$ | $\epsilon_2/\epsilon_o$ | $\epsilon_3/\epsilon_o$ | $\epsilon_1/\epsilon_o$ | $\epsilon_2/\epsilon_o$ | $\epsilon_3/\epsilon_o$ | $\epsilon_4/\epsilon_o$ |
| $\delta \to 0$ | $1/(3\,\delta)$ | $(2\,\delta)/3$ | $6\delta$ | $6/(10\,\delta)$ | $(6\delta)/10$ | $1/(10\delta)$ | $3\,\delta$ | $5/(7\delta)$ | $(4\delta)/7$ |
| 0.001 | 333.501 | 0.000665669 | 0.00599693 | 600.896 | 0.000598504 | 100.053 | 0.00299556 | 716.069 | 0.000569436 |
| 0.0025 | 133.502 | 0.00166045 | 0.0149802 | 240.89 | 0.00149069 | 40.0583 | 0.00747285 | 287.493 | 0.00141619 |
| 0.005 | 66.8382 | 0.00330864 | 0.0299163 | 120.881 | 0.00296304 | 20.0666 | 0.0148952 | 144.629 | 0.00280808 |
| 0.01 | 33.5097 | 0.00656906 | 0.0596308 | 60.8614 | 0.00585428 | 10.0833 | 0.0296111 | 73.1875 | 0.00552166 |
| 0.025 | 13.5243 | 0.0160781 | 0.147067 | 24.804 | 0.0141267 | 4.1329 | 0.0730927 | 30.2898 | 0.0131449 |
| 0.05 | 6.88167 | 0.0311111 | 0.284468 | 12.7124 | 0.0267313 | 2.21349 | 0.145215 | 15.9343 | 0.024375 |
| 0.1 | 3.59547 | 0.0586908 | 0.514842 | 6.56045 | 0.0484269 | 1.35828 | 0.293044 | 8.64352 | 0.0426822 |

TABLE II
2D RELATIVE PERMITTIVITIES FOR $0.1R$ BOUNDARY STACK-UP WITH DIRICHLET OUTER BOUNDARY.

| N | $\delta$ | $\epsilon_1/\epsilon_0$ | $\epsilon_2/\epsilon_0$ | $\epsilon_3/\epsilon_0$ | $\epsilon_4/\epsilon_0$ | $\epsilon_5/\epsilon_0$ | $\epsilon_6/\epsilon_0$ | $\epsilon_7/\epsilon_0$ | $\epsilon_8/\epsilon_0$ | $\epsilon_9/\epsilon_0$ | $\epsilon_{10}/\epsilon_0$ |
|---|---|---|---|---|---|---|---|---|---|---|---|
| 1 | $\frac{1}{10}$ | 0.0950226 | | | | | | | | | |
| 2 | $\frac{1}{20}$ | 6.88167 | 0.0311111 | | | | | | | | |
| 3 | $\frac{1}{30}$ | 0.194197 | 18.7726 | 0.0184821 | | | | | | | |
| 4 | $\frac{1}{40}$ | 4.1329 | 0.0730927 | 30.2898 | 0.0131449 | | | | | | |
| 5 | $\frac{1}{50}$ | 0.288508 | 10.8586 | 0.0458772 | 41.5572 | 0.0101984 | | | | | |
| 6 | $\frac{1}{60}$ | 2.99677 | 0.11082 | 17.2721 | 0.0338143 | 52.7245 | 0.00833053 | | | | |
| 7 | $\frac{1}{70}$ | 0.377373 | 7.72003 | 0.0694494 | 23.3195 | 0.0268835 | 63.8397 | 0.00704076 | | | |
| 8 | $\frac{1}{80}$ | 2.38424 | 0.148376 | 12.3865 | 0.0515218 | 29.1926 | 0.0223527 | 74.9238 | 0.00609673 | | |
| 9 | $\frac{1}{90}$ | 0.459734 | 5.97251 | 0.0918638 | 16.7005 | 0.0412586 | 34.9645 | 0.0191478 | 85.9879 | 0.00537587 | |
| 10 | $\frac{1}{100}$ | 2.00711 | 0.186762 | 9.71645 | 0.0680432 | 20.832 | 0.0345348 | 40.6719 | 0.0167565 | 97.0386 | 0.00480743 |

TABLE III
HIGHER ORDER 2D SOLUTIONS WITH NEUMANN OUTER BOUNDARY.

| $\delta$ | 2rd Order | | 3rd Order | | | 4th Order | | | |
|---|---|---|---|---|---|---|---|---|---|
| | $\epsilon_1/\epsilon_o$ | $\epsilon_2/\epsilon_o$ | $\epsilon_1/\epsilon_o$ | $\epsilon_2/\epsilon_o$ | $\epsilon_3/\epsilon_o$ | $\epsilon_1/\epsilon_o$ | $\epsilon_2/\epsilon_o$ | $\epsilon_3/\epsilon_o$ | $\epsilon_4/\epsilon_o$ |
| $\delta \to 0$ | $3\,\delta$ | $3/(2\,\delta)$ | $1/(6\delta)$ | $(10\,\delta)/6$ | $10/(6\delta)$ | $10\delta$ | $1/(3\delta)$ | $(7\delta)/5$ | $7/(4\delta)$ |
| 0.001 | 0.00299849 | 1502.25 | 166.752 | 0.00166418 | 1670.83 | 0.00999467 | 333.827 | 0.00139651 | 1756.12 |
| 0.0025 | 0.0074905 | 602.245 | 66.755 | 0.00415127 | 670.829 | 0.0249636 | 133.818 | 0.00347834 | 706.12 |
| 0.005 | 0.0149615 | 302.239 | 33.4266 | 0.00827262 | 337.491 | 0.049834 | 67.1355 | 0.00691422 | 356.115 |
| 0.01 | 0.0298421 | 152.229 | 16.7699 | 0.0164308 | 170.815 | 0.0991743 | 33.7712 | 0.0136635 | 181.105 |
| 0.025 | 0.0739412 | 62.1965 | 6.79961 | 0.0403162 | 70.7882 | 0.241961 | 13.6813 | 0.0330144 | 76.075 |
| 0.05 | 0.145314 | 32.1429 | 3.51534 | 0.0786636 | 37.4093 | 0.451776 | 6.88636 | 0.0627577 | 41.0256 |
| 0.1 | 0.278128 | 17.0384 | 1.94234 | 0.152429 | 20.6497 | 0.736225 | 3.41246 | 0.115694 | 23.429 |

TABLE IV
2D RELATIVE PERMITTIVITIES FOR $0.1R$ BOUNDARY STACK-UP WITH NEUMANN OUTER BOUNDARY.

| N | $\delta$ | $\epsilon_1/\epsilon_0$ | $\epsilon_2/\epsilon_0$ | $\epsilon_3/\epsilon_0$ | $\epsilon_4/\epsilon_0$ | $\epsilon_5/\epsilon_0$ | $\epsilon_6/\epsilon_0$ | $\epsilon_7/\epsilon_0$ | $\epsilon_8/\epsilon_0$ | $\epsilon_9/\epsilon_0$ | $\epsilon_{10}/\epsilon_0$ |
|---|---|---|---|---|---|---|---|---|---|---|---|
| 1 | $\frac{1}{10}$ | 10.5238 | | | | | | | | | |
| 2 | $\frac{1}{20}$ | 0.145314 | 32.1429 | | | | | | | | |
| 3 | $\frac{1}{30}$ | 5.1494 | 0.053269 | 54.1064 | | | | | | | |
| 4 | $\frac{1}{40}$ | 0.241961 | 13.6813 | 0.0330144 | 76.075 | | | | | | |
| 5 | $\frac{1}{50}$ | 3.46611 | 0.0920926 | 21.7973 | 0.0240632 | 98.0545 | | | | | |
| 6 | $\frac{1}{60}$ | 0.333693 | 9.02367 | 0.057897 | 29.5733 | 0.0189665 | 120.04 | | | | |
| 7 | $\frac{1}{70}$ | 2.6499 | 0.129533 | 14.399 | 0.0428826 | 37.1975 | 0.0156642 | 142.03 | | | |
| 8 | $\frac{1}{80}$ | 0.419421 | 6.73965 | 0.0807328 | 19.4093 | 0.0342553 | 44.7374 | 0.0133469 | 164.022 | | |
| 9 | $\frac{1}{90}$ | 2.17517 | 0.167434 | 10.8857 | 0.0598784 | 24.2374 | 0.0286004 | 52.2252 | 0.0116295 | 186.016 | |
| 10 | $\frac{1}{100}$ | 0.498229 | 5.35441 | 0.102918 | 14.6965 | 0.0480031 | 28.9563 | 0.024587 | 59.6785 | 0.0103052 | 208.011 |

where $m = 1 \ldots N$ indexes the layers in the boundary region and

$$u_n = c_{m1}(n)\rho^n + c_{m2}(n)\rho^{-(n+1)} \tag{27}$$

Eqs. (11)-(15) still apply for determining the $c_{m1}$ and $c_{m2}$ constants for a given $n$, $\delta$, and $\epsilon_1 \ldots \epsilon_m$. However, because of the slightly different form of (25) versus (8), the equations that must be solved to determine the permittivities are:

$$\frac{\epsilon_1}{\epsilon_o} \frac{\partial V_{1,n}}{\partial \rho}(R) + \frac{(n+1)V_{1,n}(R)}{R} = 0 \text{ for } n = 0 \ldots (N-1) \tag{28}$$

Numerical methods similar to those previously described for the 2D planar case can be used to solve for axisymmetric IABC permittivities. Again, for the $N = 1$ case, there are analytical solutions. For the Dirichlet outer boundary case, the solution is:

$$\frac{\epsilon_1}{\epsilon_0} = \frac{\delta}{1+\delta} \approx \delta \tag{29}$$

For the Neumann outer boundary case, there is no solution if the $n = 0$ harmonic is retained. In (28), $n = 1 \ldots N$ instead of starting with zero. For the $N = 1$ Neumann outer boundary, the analytical solution is:

$$\frac{\epsilon_1}{\epsilon_0} = \frac{\delta^3 + 3\delta^2 + 3\delta + 3}{\delta\left(\delta^2 + 3\delta + 3\right)} \approx \frac{1}{\delta} \tag{30}$$

The numerical solutions for permittivity for higher order axisymmetric IABCs are presented in Tables V and VII. The permittivities necessary to implement axisymmetric IABCs with a $R/10$ total boundary region thickness are presented in Tables VI and VIII.

For the axisymmetric case, the relative permittivities for the Neumann case are *not* the reciprocals of the Dirichlet case. Again, this result can be understood by appealing to electric vector potential. Eq. (22) describes the axisymmetric case as well. However, in the axisymmetric case, the nonzero element is $T_\theta$, the polar-directed component of electric vector potential. Similar to axisymmetric magnetic problems [5], the axisymmetric version of (22) written in terms of a cylindrical coordinate system defined by radius $r$ and axial position $z$ is:

$$-\frac{1}{\epsilon}\left\{\frac{\partial^2 T_\theta}{\partial z^2} + \frac{\partial}{\partial r}\left(\frac{1}{r}\frac{\partial r T_\theta}{\partial r}\right)\right\} = 0 \tag{31}$$

For comparison, the axisymmetric version of (6) is:

$$-\epsilon\left\{\frac{\partial^2 V}{\partial z^2} + \frac{1}{r}\frac{\partial}{\partial r}\left[r\frac{\partial V}{\partial r}\right]\right\} = 0 \tag{32}$$

Although a consideration of (31) with a $T_\theta = 0$ boundary condition would produce the permittivities necessary for the Neumann boundary scalar potential IABC, (31) and (32) are fundamentally different operators. In addition, a different set of harmonics are considered. The $n = 0$ harmonic is considered for the Dirichlet version, whereas the lowest order harmonic for the Neumann case is $n = 1$. Because the differential operators and harmonic under consideration are different, the relative permittivities in the Neumann and Dirichlet cases are not reciprocals.

## V. SCALAR POTENTIAL OPEN BOUNDARY EXAMPLES

### A. 2D Example

A good 2D open boundary example is the determination the per-unit-length capacitance of round parallel wires of different diameter. A specific example that appears in both [10] and [11] assumes wire radii of 2 cm and 4 cm with a center-to-center separation of 14 cm. For this case, a capacitance of 18.01 pF/m is expected from the analytical solution given in [11]. In both works, a potentials of 1V and -0.661875V are assumed for the small and large wires, respectively. This choice of potentials enforces the conservation of charge on the two conductors when $V = 0$ at infinity. However, selection of these voltages requires knowledge of the unbounded solution–these voltages could not be picked *a priori*. Instead, the present version of the example will specify 1V and 0V on the the small and large wires, respectively, in combination with a Neumann-type outer boundary. Like [10], the present example assumes an interior solution region with a radius of 13.4 cm located 2 cm from the large conductor.

The FEMM [12] finite element solver was used in this example. A $3^{rd}$ order Neumann IABC was selected to approximate an open region, using the relative permittivities listed in Table IV. A mesh of first-order triangular elements connecting 13429 node points was used for the solution. The computed voltage isoclines for the problem are shown in Figure 2. By integrating over all the elements in the problem (including those in the boundary shells), the stored energy, $W$, can be obtained via the formula:

$$W = \frac{1}{2}\int \mathbf{D} \cdot \mathbf{E} \, dv \tag{33}$$

Knowing the stored energy and the voltage difference, $\Delta V$, between the wires, the capacitance, $C$, can be obtained, through the definition of energy stored in a capacitor:

$$W = \frac{1}{2}C\Delta V^2 \tag{34}$$

The computed capacitance for this example is 18.02 pF, a
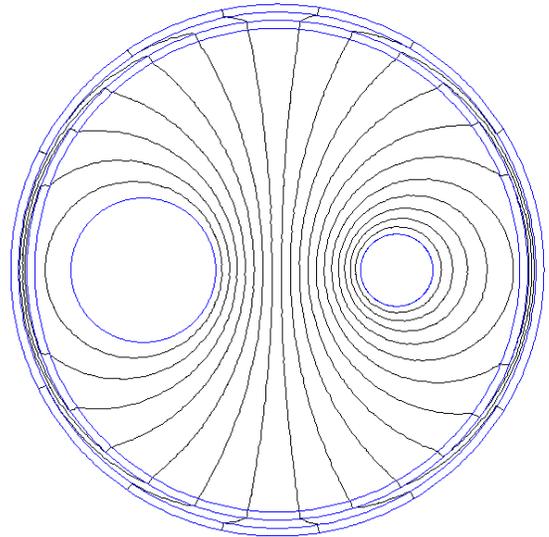


Fig. 2. Conductor capacitance example with $3^{rd}$ order Neumann IABCs.

result close to the analytical value.

TABLE V
HIGHER ORDER AXISYMMETRIC SOLUTIONS WITH DIRICHLET OUTER BOUNDARY.

| | 2rd Order | | 3rd Order | | | 4th Order | | | |
|---|---|---|---|---|---|---|---|---|---|
| $\delta$ | $\epsilon_1/\epsilon_o$ | $\epsilon_2/\epsilon_o$ | $\epsilon_1/\epsilon_o$ | $\epsilon_2/\epsilon_o$ | $\epsilon_3/\epsilon_o$ | $\epsilon_1/\epsilon_o$ | $\epsilon_2/\epsilon_o$ | $\epsilon_3/\epsilon_o$ | $\epsilon_4/\epsilon_o$ |
| $\delta \to 0$ | $1/(2\delta)$ | $\delta$ | $5\delta$ | $25/(24\delta)$ | $(5\delta)/4$ | $1/(8\delta)$ | $(23\delta)/8$ | $529/(360\delta)$ | $(23\delta)/15$ |
| 0.001 | 500.001 | 0.000997009 | 0.00499497 | 1041.67 | 0.00124378 | 125.003 | 0.00286644 | 1469.45 | 0.00152266 |
| 0.0025 | 200.003 | 0.00248139 | 0.0124683 | 416.664 | 0.00308636 | 50.0075 | 0.00713468 | 587.783 | 0.00376722 |
| 0.005 | 100.005 | 0.00492611 | 0.0248715 | 208.327 | 0.0060971 | 25.015 | 0.014168 | 293.899 | 0.00740601 |
| 0.01 | 50.01 | 0.00970878 | 0.0494723 | 104.155 | 0.0119013 | 12.5301 | 0.027955 | 146.965 | 0.0143199 |
| 0.025 | 20.0252 | 0.0232571 | 0.12146 | 41.6379 | 0.0277329 | 5.07522 | 0.0674798 | 58.8308 | 0.0324964 |
| 0.05 | 10.0505 | 0.0434961 | 0.234418 | 20.7791 | 0.0497316 | 2.6494 | 0.129375 | 29.4945 | 0.0560798 |
| 0.1 | 5.10097 | 0.0771322 | 0.429378 | 10.3276 | 0.0820837 | 1.5363 | 0.2472 | 14.892 | 0.0872062 |

TABLE VI
AXISYMMETRIC RELATIVE PERMITTIVITIES FOR $0.1R$ BOUNDARY STACK-UP WITH DIRICHLET OUTER BOUNDARY.

| $N$ | $\delta$ | $\epsilon_1/\epsilon_0$ | $\epsilon_2/\epsilon_0$ | $\epsilon_3/\epsilon_0$ | $\epsilon_4/\epsilon_0$ | $\epsilon_5/\epsilon_0$ | $\epsilon_6/\epsilon_0$ | $\epsilon_7/\epsilon_0$ | $\epsilon_8/\epsilon_0$ | $\epsilon_9/\epsilon_0$ | $\epsilon_{10}/\epsilon_0$ |
|---|---|---|---|---|---|---|---|---|---|---|---|
| 1 | $\frac{1}{10}$ | 0.0909091 | | | | | | | | | |
| 2 | $\frac{1}{20}$ | 10.0505 | 0.0434961 | | | | | | | | |
| 3 | $\frac{1}{30}$ | 0.16015 | 31.2123 | 0.0356179 | | | | | | | |
| 4 | $\frac{1}{40}$ | 5.07522 | 0.0674798 | 58.8308 | 0.0324964 | | | | | | |
| 5 | $\frac{1}{50}$ | 0.249837 | 13.9595 | 0.0485094 | 93.6268 | 0.0308341 | | | | | |
| 6 | $\frac{1}{60}$ | 3.43867 | 0.100076 | 23.6832 | 0.0405888 | 135.819 | 0.0298002 | | | | |
| 7 | $\frac{1}{70}$ | 0.338611 | 9.11831 | 0.0674884 | 34.5315 | 0.0362401 | 185.492 | 0.0290973 | | | |
| 8 | $\frac{1}{80}$ | 2.63643 | 0.134865 | 15.0974 | 0.0539561 | 46.7532 | 0.0334921 | 242.665 | 0.0285874 | | |
| 9 | $\frac{1}{90}$ | 0.422731 | 6.77301 | 0.0874553 | 21.3014 | 0.0465142 | 60.4415 | 0.0316000 | 307.363 | 0.0282013 | |
| 10 | $\frac{1}{100}$ | 2.16756 | 0.171316 | 11.1989 | 0.0680376 | 27.9482 | 0.0418045 | 75.638 | 0.0302177 | 379.587 | 0.0278984 |

TABLE VII
HIGHER ORDER AXISYMMETRIC SOLUTIONS WITH NEUMANN OUTER BOUNDARY.

| | 2rd Order | | 3rd Order | | | 4th Order | | | |
|---|---|---|---|---|---|---|---|---|---|
| $\delta$ | $\epsilon_1/\epsilon_o$ | $\epsilon_2/\epsilon_o$ | $\epsilon_1/\epsilon_o$ | $\epsilon_2/\epsilon_o$ | $\epsilon_3/\epsilon_o$ | $\epsilon_1/\epsilon_o$ | $\epsilon_2/\epsilon_o$ | $\epsilon_3/\epsilon_o$ | $\epsilon_4/\epsilon_o$ |
| $\delta \to 0$ | $4\delta$ | $2/\delta$ | $1/(7\delta)$ | $(120\delta)/49$ | $20/(7\delta)$ | $12\delta$ | $6/(19\delta)$ | $(840\delta)/361$ | $70/(19\delta)$ |
| 0.001 | 0.00399599 | 2000. | 142.86 | 0.00244168 | 2857.15 | 0.0119875 | 315.784 | 0.0023153 | 3684.22 |
| 0.0025 | 0.00997481 | 800. | 57.1495 | 0.00607731 | 1142.87 | 0.029917 | 126.301 | 0.00574554 | 1473.71 |
| 0.005 | 0.0198985 | 400. | 28.5848 | 0.0120674 | 571.45 | 0.0596363 | 63.1283 | 0.011352 | 736.9 |
| 0.01 | 0.0395883 | 200. | 14.3124 | 0.0238035 | 285.757 | 0.118297 | 31.5204 | 0.0221718 | 368.536 |
| 0.025 | 0.0973252 | 79.9991 | 5.78115 | 0.0573497 | 114.392 | 0.285096 | 12.4933 | 0.051874 | 147.652 |
| 0.05 | 0.188706 | 39.9975 | 2.99018 | 0.109309 | 57.3539 | 0.518654 | 6.08207 | 0.0943175 | 74.2362 |
| 0.1 | 0.351313 | 19.9973 | 1.68571 | 0.205825 | 28.9765 | 0.801713 | 2.88849 | 0.163862 | 37.8756 |

TABLE VIII
AXISYMMETRIC RELATIVE PERMITTIVITIES FOR $0.1R$ BOUNDARY STACK-UP WITH NEUMANN OUTER BOUNDARY.

| $N$ | $\delta$ | $\epsilon_1/\epsilon_0$ | $\epsilon_2/\epsilon_0$ | $\epsilon_3/\epsilon_0$ | $\epsilon_4/\epsilon_0$ | $\epsilon_5/\epsilon_0$ | $\epsilon_6/\epsilon_0$ | $\epsilon_7/\epsilon_0$ | $\epsilon_8/\epsilon_0$ | $\epsilon_9/\epsilon_0$ | $\epsilon_{10}/\epsilon_0$ |
|---|---|---|---|---|---|---|---|---|---|---|---|
| 1 | $\frac{1}{10}$ | 10.0634 | | | | | | | | | |
| 2 | $\frac{1}{20}$ | 0.188706 | 39.9975 | | | | | | | | |
| 3 | $\frac{1}{30}$ | 4.37479 | 0.075118 | 85.8557 | | | | | | | |
| 4 | $\frac{1}{40}$ | 0.285096 | 12.4933 | 0.051874 | 147.652 | | | | | | |
| 5 | $\frac{1}{50}$ | 3.06077 | 0.112378 | 22.0265 | 0.0423167 | 225.43 | | | | | |
| 6 | $\frac{1}{60}$ | 0.374816 | 8.17242 | 0.0740027 | 33.0192 | 0.0371234 | 319.234 | | | | |
| 7 | $\frac{1}{70}$ | 2.40892 | 0.149299 | 13.8176 | 0.0582172 | 45.656 | 0.0338673 | 429.046 | | | |
| 8 | $\frac{1}{80}$ | 0.457719 | 6.15238 | 0.0951954 | 19.795 | 0.0495821 | 60.002 | 0.0316392 | 554.889 | | |
| 9 | $\frac{1}{90}$ | 2.01871 | 0.187242 | 10.323 | 0.0732287 | 26.2901 | 0.0441395 | 76.0845 | 0.0300195 | 696.75 | |
| 10 | $\frac{1}{100}$ | 0.533241 | 4.9312 | 0.116425 | 14.5221 | 0.0612364 | 33.375 | 0.0403993 | 93.9198 | 0.028790 | 854.64 |

## B. 2D Scalar Magnetostatics Example

The as noted in the Introduction, the techniques developed in this work can be applied to any scalar potential formulation. As an example of the application of the boundary condition to other scalar potential problem types, a 2D planar magnetic problem with a scalar magnetic formulation will be considered. At low frequency, if permanent magnets are the only field source, the magnetic field is described by a subset of Maxwell's equations:

$$\nabla \cdot \mathbf{B} = 0 \tag{35}$$

$$\nabla \times \mathbf{H} = 0 \tag{36}$$

where $\mathbf{H}$ is the magnetic field intensity; $\mathbf{B}$ is the magnetic flux density. To include the effects of the permanent magnets, flux density can be defined as [13]:

$$\mathbf{B} = \mu \mathbf{H} + \mathbf{B}_r \tag{37}$$

where $\mu$ is the magnetic permeability and $\mathbf{B}_r$ is the remanence of the permanent magnet material.

The magnetic field can be defined in terms of magnetic scalar potential potential, $\Omega$ as:

$$\mathbf{H} = -\nabla \Omega \tag{38}$$

This definition of magnetic potential uniformly satisfies (36). Substituting (38) and (37) yields:

$$\nabla \cdot \mathbf{B} = -\nabla \cdot \mu \nabla \Omega + \nabla \cdot \mathbf{B}_r = 0 \tag{39}$$

Re-arranging, (39) can be written as:

$$-\nabla \cdot \mu \nabla \Omega = \rho_m \tag{40}$$

where $\rho_m$ is the magnetic charge density defined as:

$$\rho_m = -\nabla \cdot \mathbf{B}_r \tag{41}$$

In the "far field" region, the material is free space ($\mu = \mu_o$, the permeability of free space) and there is no magnetic material, so (40) simplifies to:

$$-\mu_o \nabla^2 \Omega = 0 \tag{42}$$

Comparing (40) to (5), the equations have exactly the same form. The electrostatic and magnetostatic problems are analogous, with $\mathbf{B}$, $\mathbf{H}$, $\mu$ and $\Omega$ analogous to $\mathbf{D}$, $\mathbf{E}$, $\epsilon$ and $V$ respectively. The Improvised Asymptotic boundary can therefore be used by defining the relative permeability of the circular shells represented the unbounded external region in a scalar potential magnetic problem to be the same as the relative permittivity in circular shells of the analogous electrostatic problem. Since magnetic problems naturally conserve source charges but do not naturally define potential at any point in the near field, a Dirichlet outer boundary is appropriate for this problem.

The goal is to compute the torque on a 15 mm × 5 mm × 10 mm bar magnet when the magnet is placed in a uniform external magnetic field. For the purposes of the example, the magnet is magnetized along the direction of the 15 mm dimension. The magnet is assumed to be an ideal 42 MGOe magnet with remanence $B_r = 1.29615$ T and coercivity

$H_c = 1,031,442$ A/m (*i.e.* straight-line demagnetization curve with a slope of $\mu_o$). The external field, $B_{ext}$, is 0.1 T in magnitude and directed perpendicular to the magnetization direction of the magnet.

This problem has a straightforward analytical solution [14]:

$$\tau = \mathbf{m} \times \mathbf{B} \tag{43}$$

where $\tau$ is torque, $\mathbf{m}$ is a vector representing the magnet's dipole moment. Since the magnet has ideal properties, the magnitude of dipole moment is $H_c$ times the volume of the magnet:

$$\mathbf{m} = (0.773581 \, \text{A*m}^2) * \mathbf{j} \tag{44}$$

A vector indicating the direction and magnitude of the external field is:

$$\mathbf{B}_{ext} = (0.1 \, \text{T}) * \mathbf{i} \tag{45}$$

From (43), the analytically calculated value for torque is:

$$\tau = (-77.36 \, \text{N*mm}) * \mathbf{k} \tag{46}$$

where $\mathbf{i}$, $\mathbf{j}$ and $\mathbf{k}$ represent orthogonal unit vectors.

The first step in creating the numerical solution is to establish the constant external magnetic field $\mathbf{B}_{ext}$ that exists in the absence of the magnet. As is noted in [15], for an ideal infinitely long diametrically magnetized cylinder, the flux density inside the magnet is equal to $B_r/2$. The uniform magnetic field can therefore be created by drawing a domain with radius $R = 10$ mm. At $R$, a magnetic surface charge distribution, $\rho_m$, can be imposed to create the uniform magnetic field:

$$\rho_m = -2B_{ext}\cos\phi \tag{47}$$

To establish the proper field, unbounded space can be modeled by creating an IABC. In this case, a third-order IABC is selected with $\delta = 1/30$ with the permeabilities for each layer prescribed by Table II. In this case, the charge specified by (47) clearly integrates to zero over the domain, and no fixed potential is defined elsewhere. The Dirichlet IABC is needed here to obtain a unique solution. The result is an even magnetic field of $B_{ext}$ in the region of interest. To model this configuration, the FEMM electrostatics solver was again employed, interpreting the $\mathbf{D}$, $\mathbf{E}$, and $\epsilon$ as their magnetic analogs, magnetic flux density $\mathbf{B}$, magnetic field intensity $\mathbf{H}$, and magnetic permeability $\mu$. The resulting field distribution is pictured in Figure 3.

The lines in Figure 3 are lines of constant magnetic potential; flux density flows normal to the isoclines, as indicated in the Figure.

The permanent magnet can then be modeled by placing a magnetic surface charge distribution of $B_r$ on the magnet's North pole and $-B_r$ at the magnet's South pole. The resulting solution, without the superimposed constant $B_{ext}$ field, is shown as Figure 4. Again, the lines in the Figure indicate magnetic potential isoclines and flux outside the magnet flows perpendicular to these lines.

The combined uniform and permanent magnet fields are shown in Figure 5. A first-order triangular mesh of about 5600 nodes was used to create the solution shown in Figure 5. The Eggshell Method [16] was used to evaluate Maxwell's stress
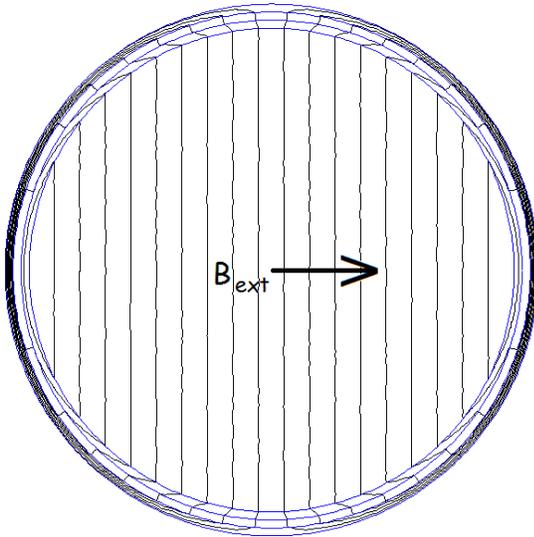
Fig. 3. Constant magnetic field with $3^{rd}$ order Dirichlet IABCs.
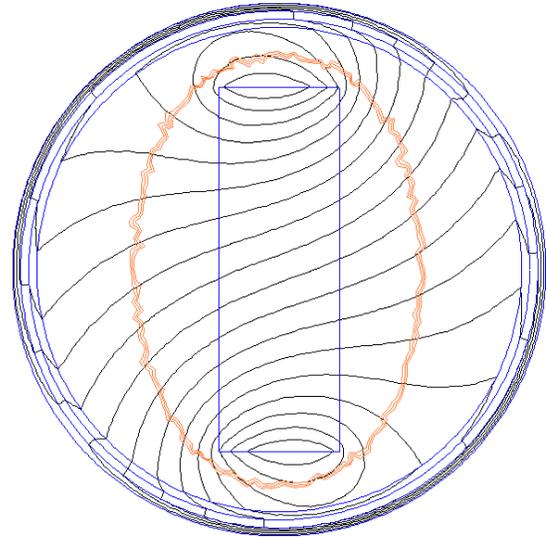


Fig. 5. Combined constant field / bar magnet solution.
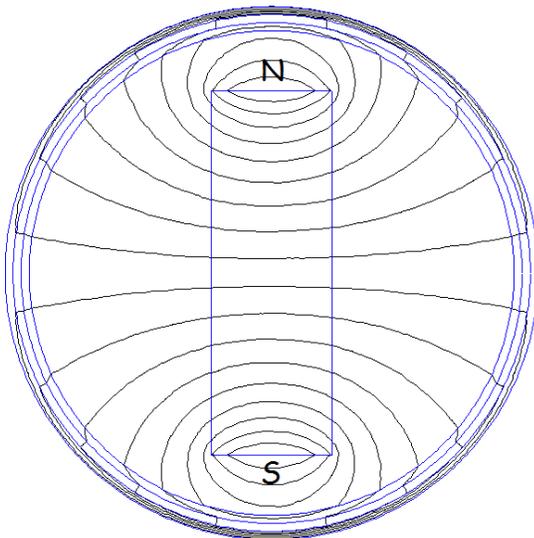


Fig. 4. Bar magnet and $3^{rd}$ order Dirichlet IABCs.

tensor over a volume rather than over a surface. The oval of lines on the Figure encircling the magnet indicate a row of elements over which the torque was evaluated via the Eggshell Method. The torque computed by finite element analysis is -77.33 N*mm, a result close to the analytical calculation.

### C. Axisymmetric Example

A simple but illustrative axisymmetric example is a charged, conductive sphere in unbounded space. For this example, a Dirichlet-type IABC must be used so that charge on the sphere is balanced by charges "at infinity". In this particular case, a sphere with a voltage of $V_o$ and a radius of $R_s = 0.5$ m is considered. For the purposes of this analysis, the computational domain is truncated to $R = 1$ m. Various orders of IABCs are then applied to the problem. The thickness of the layers is selected so that for the $N^{th}$ order IABC, $\delta * N = 0.1$. With this selection of thickness, all solutions are solved over the

same domain size and have approximately the same number of elements. The relative permittivities used in the construction of the IABCs in the example are listed in Table VI.

This example has simple solutions for both voltage as a function of position and capacitance [14]:

$$V(\rho, \phi) = V_o \frac{R_s}{\rho} \tag{48}$$

$$C = 4\pi\epsilon_0 R_s = 55.6325 \, \text{pF} \tag{49}$$

In each solution, about 35,000 node points were used. In the centered position, the finite element solver computes a capacitance of $55.6335 \pm 0.0001$ pF for the IABC cases. The small difference between the analytical and FEA solutions is due to discretization error and to approximation of the circular surfaces of the sphere and boundary by polygons with sides that span one degree of the surface per side. If an open boundary scheme is effective, the capacitance should be insensitive to the position of the sphere within the computational domain. For example, the left plot in Figure 6 shows the level contours of voltage for a centered sphere with an artificial outer boundary at $\rho = 2R$ fixed to $V_o/2$. This plot represents the analytical solution for the case of a centered sphere. The right plot in Figure 6 shows a $3^{rd}$ order improvised asymptotic boundary condition solution. However, the sphere has been displaced by $0.8R$ from the centered position. It can be observed that the voltage isoclines in the IABC plot still form circles about the boundary of the sphere and appear to be unaffected by the position of the sphere within the domain.

Figure 7 shows a plot of change in computed capacitance versus position for different orders of improvised ABCs. The first-order IABC is fairly sensitive to position. However, the higher order IABCs are increasingly insensitive to the position of the sphere. For the higher-order BCs, the error is dominated by discretization error over most of the range of travel.
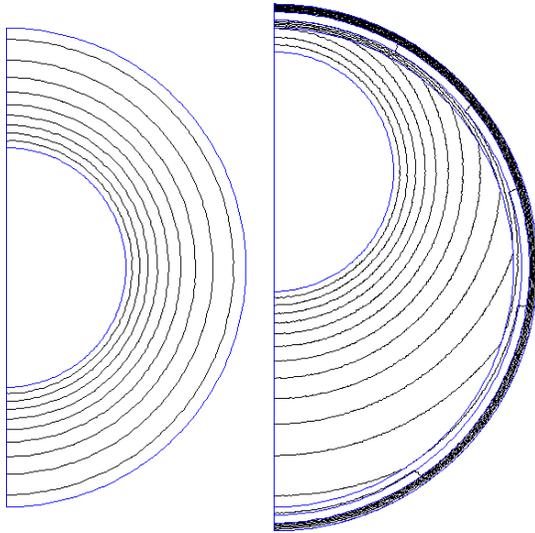
Fig. 6.  Voltage isoclines for a sphere with $3^{rd}$ order Dirichlet IABCs.
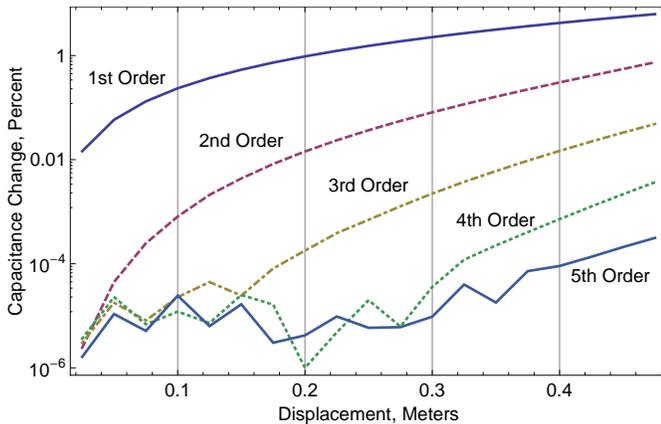


Fig. 7.  Variation in capacitance vs position for different order IABCs.

## VI. CONCLUSIONS

This paper has presented an Improvised Asymptotic Boundary Condition method to address electrostatic and related scalar potential problems. Axisymmetric and 2D examples demonstrate the use of the formulation for both the "insulated at infinity" and "grounded at infinity" problem types. Although the development in this work did not consider 3D problems directly, the axisymmetric IABCs can be applied in the 3D case as well, since the spherical shell structure derived for the axisymmetric case has no particular orientation dependence.

Although this work specifically addresses the scalar potential, the results have a broader applicability, extending to vector potential formulations as well. In Sections III and IV, the duality between scalar potential solutions with a Neumann and an analogous electric vector potential formulation with a Dirichlet outer boundary was made. Because the form of the electrostatic vector potential equations is identical to the form of magnetic vector potential equations, the relative permittivities listed in Tables III and IV for the 2D case and Tables VII and VIII can be used as the relative permeabilities in 2D and axisymmetric vector potential problems with $A = 0$

applied at the outer boundary, allowing up to $10^{th}$ order IABCs to be implemented in the vector potential case.

Future extensions to this work might explore applications of IABCs non-circular boundaries or non-static problems.

### REFERENCES

[1] Q. Chen and A. Konrad, "A review of finite element open boundary techniques for static and quasi-static electromagnetic field problems," *IEEE Trans. Magn.*, vol. 33, pp. 663–676, Jan. 1997.

[2] Q. Chen, A. Konrad, and P. P. Biringer, "Computation of static and quasistatic electromagnetic fields using asymptotic boundary conditions," *Applied Computational Electromagnetics Society Journal*, vol. 9, pp. 37–42, July 1994.

[3] S. Gratkowski *et al.*, "Asymptotic boundary conditions for the finite element modeling of axisymmetric electrical field problems," *IEEE Trans. Magn.*, vol. 36, pp. 717-721, July 2000.

[4] D. Meeker, "Improvised open boundary conditions for magnetic finite elements," *IEEE Trans. Magn.*, vol. 49, pp. 5243-5247, Oct. 2013.

[5] R. Hoole, "Computer-aided analysis and design of electromagnetic devices," Elsevier, 1989.

[6] M. Stone and P. Goldbart, "Mathematics for Physics," Cambridge University Press, 2009.

[7] J. Lekner, "Electrostatic force between two conducting spheres at constant potential difference," *J. Appl. Phys.*, vol. 111, 076102, 2012.

[8] R. Haberman, *Elementary Applied Partial Differential Equations*, 2nd ed., Prentice-Hall, 1987.

[9] J. D. Jackson, *Classical Electrodynamics*, 3rd ed., Wiley, 1999.

[10] L. Dedek, J. Dedkova, and J. Valsa, "Optimization of perfectly matched layer for Laplace's equation," *IEEE Trans. Magn.*, vol. 38, pp. 501–504, Mar. 2002.

[11] S. Alfonzetti, G. Borz, and N. Salerno, "Some considerations about the perfectly matched layer for static fields," *COMPEL*, vol. 18, pp. 337–347, 1999.

[12] D. C. Meeker, *Finite Element Method Magnetics*, Version 4.2 (25Aug2013 Build), http://www.femm.info

[13] O. Biro et al., "Computation of 3-D magnetostatic fields using a reduced scalar potential," *IEEE Trans. Magn.*, vol. 29, pp. 1329–1332, Mar. 1993.

[14] M. Plonus *Applied electromagnetics*, McGraw-Hill, 1978.

[15] S. Chikazumi, *Physics of Ferromagnetism*, 2nd ed., Oxford University Press, 1997.

[16] F. Henrotte, G. Delige, K. Hameyer, "The eggshell approach for the computation of electromagnetic forces in 2D and 3D", *COMPEL*, vol. 23, pp. 996–1005, 2004.

**David C. Meeker** (Member, IEEE) received the B.S. degree in mechanical engineering from Duke University, Durham, NC, in 1990 and the M.S. and Ph.D. degrees in mechanical and aerospace engineering from the University of Virginia, Charlottesville, in 1993 and 1996, respectively. Since 1998, he has worked on the design, analysis, and control of novel electric machines as a Senior Scientist at QinetiQ North America in Waltham, MA. He is also the author of the magnetics finite element analysis program FEMM, which has been used by various authors in more than 100 IEEE publications.